

Review

Approaching the Black Hole by Numerical Simulations

Christian Fendt 

Max Planck Institute for Astronomy, Königstuhl 17, D-69117 Heidelberg, Germany; fendt@mpia.de

Received: 2 February 2019; Accepted: 23 April 2019; Published: 29 April 2019



Abstract: Black holes represent extreme conditions of physical laws. Predicted about a century ago, they are now accepted as astrophysical reality by most of the scientific community. Only recently has more direct evidence of their existence been found—the detection of gravitational waves from black hole mergers and of the shadow of a supermassive black hole in the center of a galaxy. Astrophysical black holes are typically embedded in an active environment which is affected by the strong gravity. When the environmental material emits radiation, this radiation may carry imprints of the black hole that is hosting the radiation source. In order to understand the physical processes that take place in the close neighborhood of astrophysical black holes, numerical methods and simulations play an essential role. This is simply because the dynamical evolution and the radiative interaction are far too complex in order to allow for an analytic solution of the physical equations. A huge progress has been made over the last decade(s) in the numerical code development, as well as in the computer power that is needed to run these codes. This review tries to summarize the basic questions and methods that are involved in the undertaking of investigating the astrophysics of black holes by numerical means. It is intended for a non-expert audience interested in an overview over this broad field. The review comes along without equations and thus without a detailed expert discussion of the underlying physical processes or numerical specifics. Instead, it intends to illustrate the richness of the field and to motivate further reading. The review puts some emphasis on magneto-hydrodynamic simulations but also touches radiation transfer and merger simulations, in particular pointing out differences in these approaches.

Keywords: black hole; computational astrophysics; magneto-hydrodynamics, radiation transport; relativity; accretion disks; jets; merger; gravitational waves; active galactic nuclei; micro quasars

1. Introduction

For many people—both scientists and the public—black holes are considered as the most fascinating objects in the universe. In principle, black holes simply consist of highly compressed and invisible mass, solely described by its mass and angular momentum, and are thus physically and chemically less rich compared to e.g., the solar atmosphere. However, the compactness of the accumulated mass distorts the surrounding space-time in such a way that the physical processes occurring close to a black hole seem to behave in contradiction to the every-day experience.

A prime mystery is (and may remain) the interior of a black hole—nobody knows how the innermost parts of a black hole are structured as we do not yet understand the physics at work under such extreme conditions. Below the black hole *horizon*, the time and space coordinates change their meaning, which may impact our common understanding of causality. In order to understand the very center—if it exists—the extreme physical conditions would ask for a new theory of physics, that is, quantum gravity, the combination of general relativity and quantum physics.

Astrophysical black holes come in various manifestations—from stellar mass black holes that can sometimes be observed as micro-quasars [1] to *supermassive* black holes that reside in the nuclei of

active galaxies and weigh up to billions of solar masses [2,3]. Intermediate mass black holes weighing some 1000s of solar masses—are discussed but not yet confirmed. Recently, by their emission of gravitational waves, a new flavor of black holes has been discovered rather unexpectedly—black holes with masses of 30–50 solar masses for which the origin is not yet known.

Astrophysical black holes do not exist alone in space but are surrounded by other material that is moving with high speed and is also radiating. As a consequence, we expect that certain features of this radiation may carry along characteristic imprints of the black hole from where it originated.

This review wants to touch on three basic questions of black hole physics that can be addressed by using numerical simulations. We want to understand (i) how the environmental material behaves dynamically when it comes close to the black hole, (ii) how that material looks like for a distant observer, and (iii) what could be learned about the black hole parameters by comparing theoretical modeling and observational data.

In order to answer these questions, the use of numerical simulations is essential, if not inevitable. Fortunately, the availability of large computer clusters for high-performance codes has vastly increased over the recent years. In general, these codes do solve the time-dependent physical equations considering general relativistic space-time. As a result, the time-evolution of the dynamics of the matter and the electromagnetic field and also the radiation field are provided. Depending on the astrophysical context, different numerical approaches are undertaken.

One option is to concentrate on the dynamics of the material around a black hole. This is typically the accretion disk that is surrounding the supermassive black holes in the center of an active galactic nuclei or the stellar mass black holes in micro quasars. It is this *accretion disk* that makes the black hole *shine* [4]. Depending on the black hole mass and the physical radiation process, we may observe X-ray emission or UV light, emission and absorption lines, a Doppler broadening of these lines, and we may even use these lines to reconstruct the disk structure from the line signal (reverberation mapping, [5]). The same sources may eject jets—collimated and magnetized beams of high velocity that are either launched in the surrounding accretion disk [6] or by a rotating black hole itself [7]. For both processes, a strong magnetic field is essential to simulate the (magneto-)hydrodynamics of disks and outflows as well as their radiation if one of the prime targets of numerical investigations. What are the mass accretion and ejection rates, the speed and energetics of the outflows, or the accretion disk luminosity?

For a black hole located in a intensive radiation field, we may expect to observe its “shadow” against the background light as the black hole absorbs all the radiation that enters the horizon. For a long time—that means, before the recent detection of gravitational waves—for many colleagues, only the observation of the black hole shadow would have provided strong evidence for the actual existence of black holes. Numerical simulations of ray-tracing in a strong gravitational field are essential for the understanding of a (yet-to-come) observational signal of such a shadow. The idea is to compare the numerically constructed images of the area close to the black hole with the observation of nearby supermassive black hole shadow. These experiments are currently being undertaken and are focusing on the black holes with the largest angular diameter, that is, the one in the Galactic center and the one in the active galaxy M87 (see <https://eventhorizontelescope.org/>; <https://blackholecam.org/>).

Even isolated black holes may be observed if the path of light from distant sources is penetrating deep enough into the gravitational potential of a black hole that is located just between the source and the observer and thus becomes characteristically deflected (gravitational lensing; see [8,9]).

Close binary compact objects (neutron stars or black holes) will finally merge and thus strongly distort the space-time around them. This distortion propagates through space as a gravitational wave which could then be detected on Earth. As this is extremely difficult to measure, only recently could such waves be detected by the Laser Interferometer Gravitational-Wave Observatory (LIGO) gravitational wave interferometer (see <https://www.ligo.caltech.edu>). In order to interpret the observed merger signal, the numerical simulation of a merging binary system and the subsequent gravitational wave is a fundamental tool which can deliver the progenitor masses and even the distance to the gravitational wave source.

2. Numerical Approaches

In this review, we discuss the different numerical methods that were invented to investigate the close environment of black holes, considering their increasing numerical complexity. We distinguish the different approaches in three branches—these are:

- (i) Simulations mainly treating the dynamics of the black hole environment on a fixed metric;
- (ii) Simulations that ray-trace photons that are affected by strong gravity, and;
- (iii) Simulations that solve the time-dependent Einstein equations.

Of course, a combination of these approaches is possible but will be even more demanding.

In the following, we first want to briefly compare and summarize the different methods, before we go on and discuss a few technical details and exemplary results in the remaining sections.

2.1. Dynamics on Fixed Space-Time

It is considerably the most straight-forward approach to numerically evolve the environment of a black hole on a fixed space-time, thus applying a fixed metric. We may understand this approach as an analogy to the nonrelativistic treatment of gravity considering a (hydrodynamic) test mass in a Newtonian gravitational potential. The equations to be solved are the general relativistic (magneto-)hydrodynamic (MHD) equations, that is, the equation of motion defined by the time evolution of the energy–momentum–tensor on a *given* metric, fixed in time. The general approach is to choose a metric and coordinate system that are convenient for the black hole system under consideration and then solve the physical equations of interest.

A typical astrophysical prospect could be to investigate the evolution of an accretion disk or torus that is orbiting a black hole. In particular, one may investigate the stability of disks and tori, or their mass loss by accretion or the ejection of disk winds or jets. A topical motivation of this application is to learn about the feedback of supermassive black holes for cosmological galaxy formation simulations, which apply parameterized models of the energy output from galactic black holes.

The approach just described is equivalent to a nonrelativistic numerical treatment that solves the (nonrelativistic) MHD equations in the *gravitational potential* of, e.g., a star. In both cases, the surrounding masses are *test masses* affected by gravity. As such, we cannot tell from pure (magneto-)hydrodynamic simulations their astrophysical masses or the densities of the objects affected by a fixed gravity. Typically, the numerical approach gives an accretion rate in *code units* with no direct relation to an astrophysical value. However, if radiation transport is included (see below), the density scale actually matters, as absorption and emission coefficients depend on the exact physical values (see, e.g., [10,11]). Disk luminosities derived from such kinds of simulations could be directly compared to observations and can thus constrain the disk density and the mass fluxes.

Numerical simulations of the close environment of the black hole were pioneered by Wilson and collaborators [12–16]. After some years of silence—probably due to the lack of necessary computer power—the field of general relativistic time-dependent simulations flourished just after the turn of the century with a number of groups working on different numerical codes [16–24].

More physics has been added, e.g., radiation processes or a physical resistivity. Note, however, that for a number of microscopic processes, a consistent general relativistic description is missing, which may potentially lead to causality issues in the simulation (see, for example, [25,26] for the case of viscosity or conduction).

An interesting feature to note is that general relativistic magneto-hydrodynamics (GR-MHD) simulations [20,24] usually apply (modified) Kerr–Schild coordinates. In Kerr–Schild coordinates, the coordinate singularity at the horizon that is present in the Schwarzschild metric or the Kerr metric is avoided by a suitable coordinate transformation. These codes actually continue to calculate the physical evolution of the variables *inside* the horizon. Naturally, physical processes taking place inside the horizon cannot affect the (numerical) world outside the horizon. The physical conditions defined

by the horizon still apply—a neat boundary condition, which is difficult to accomplish if the horizon itself is the numerical boundary and if that boundary implies physical singularities.

A general difficulty that MHD codes have are areas of low matter density. The numerical time step decreases with increasing Alfvén speed and may “kill” the simulation. While this is a problem for nonrelativistic simulations applying strong magnetic fields and low densities, in relativistic simulations, the Alfvén speed is limited by the speed of light, and thus, the time-stepping is limited by the light-crossing time over a grid cell.

Low densities together with a strong magnetic field impose severe problems with certain variable transformations that are essential in relativistic MHD codes. Therefore, relativistic simulations consider a numerical floor model for the critical areas of low density, keeping the gas density and the internal energy above a “floor” value, a chosen (local) threshold. By that, the codes can avoid to evolve into an unphysical parameter space, for example, negative densities or pressures.

Typically, the choice of the numerical floor density affects the most relativistic regions of the simulation, for example, a Poynting flux-dominated Blandford–Znajek jet (see below). For such regions, an option may be to apply general relativistic force-free electrodynamic simulations [23,27]. However, while such simulations are able to treat highly magnetized areas very well, they can hardly capture the gas dynamics.

An essential parameter for any simulation using grid codes is the numerical resolution. High spatial resolution is desirable in order to resolve the proper physical evolution. On the other hand, high resolution in an explicit code slows down the simulation because of the small numerical time step needed to ensure a causally correct propagation across the grid. A typical astrophysical context here is the evolution of hydrodynamical instabilities and turbulence, for example, magneto-rotational instability (MRI, [28]). While the simulations have made great progress towards capturing the MRI and subsequent processes, such as angular momentum transport or a direct dynamo, the simulations often fail to capture a significant dynamical range of the turbulent cascade and thus the energy dissipation on small scales. This is of course a problem that is not restricted to general relativity.

2.2. Dynamics of Interacting Compact Objects

Compared to simulations performed on a static metric as discussed above, a more general approach is to solve Einstein equations numerically and time-dependently. This procedure is obviously needed when the mass distribution in the simulation domain changes substantially in time, leading to a similar change in the metric. A typical application is the compact object merger. No fixed metric can be chosen initially—the metric is time-dependent and results from the evolution of the mass distribution. Further, the change in the metric that is propagated away in space is just known as the gravitational wave.

Same as the approach with the fixed metric discussed above, this approach also has a nonrelativistic equivalent. The example may be a typical star formation simulation of a molecular cloud collapsing under *self-gravity*. In order to evolve the simulation, after each time step, the gravitational potential of the mass distribution has to be integrated, before the motion of masses is calculated using the updated gravitational potential in the next time step.

Pioneering work on the theoretical framework for numerical general relativity considering, e.g., the mass formula for black holes, a systematic approach to solve Einstein’s equations on dynamical space-times, or even a definition of “numerical relativity” was published during the 1970s [29–32].

It took some years until seminal development of the first 3D numerical codes designed to solve the Einstein equations for general vacuum space-times succeeded in providing the evolution for the first 3D black hole space-time [33]. A major difficulty here that had to be overcome is avoiding the singularity inside the horizon or treating the boundary conditions properly for space-times. Another feature, the so-called apparent horizon becomes important—a kind of spatial boundary that at a certain time effectively acts as an event horizon. In 3D simulations, both horizons are time-dependent and may fluctuate as the simulation progresses. The difficulty is how to determine the mass inside them.

The problem of dealing with the initial data in cases of rotating black holes or distorted nonrotating black holes was treated by the authors of [34]. Constructing the initial data for a simulation is a complex task that involves solving Einstein's equations on chosen initial spatial coordinates that then has to be embedded in the 4-dimensional space-time (see, e.g., [35]). Another seminal step was to successfully treat the motion of a black hole through a numerical grid. The difficulty here is the curvature singularities contained within the black hole(s). One way to deal with it is the so-called black hole excision where all parts of the black hole interior are excluded from the computational domain and only the exterior region is evolved [36].

2.3. Radiation—Propagation of Light Close to a Black Hole

The third approach we are discussing is numerically propagating photons along space-time, i.e., doing relativistic radiation transport. What was discussed above was mainly related to the *dynamical* evolution of matter (and the magnetic field). Simulations of the dynamics deliver the time-dependent distribution of, e.g., mass density and velocity. What can be potentially *observed* is the radiation that is emitted from this material. Thus, radiation transport will be the essential step that allows to compare numerical simulations of hydrodynamics with the observed radiation pattern.

The path of light that is passing by a black hole is governed by strong gravity. The principles seem rather simple: The trajectory of light rays follows the null geodesics of the metric—the Schwarzschild metric for nonrotating black holes or the Kerr metric for rotating black holes. More complicated situations arise if the metric is time-dependent, as for example in case of merging compact stars, or if the mass distribution that is emitting and absorbing the light is changing rapidly with time.

Figure 1 shows a schematic diagram of photon paths around a black hole. The photon trajectories can be bent *around* the black hole if a photon comes within the so-called photon sphere. Figure 2 displays a 3-dimensional realization of a numerical ray-tracing procedure applied to a luminous accretion disk orbiting a Kerr black, as seen by a distant observer under different inclination angles. Obviously, a rich radiative structure emerges, including parts of the disk that are located behind the black hole and become visible by gravity.

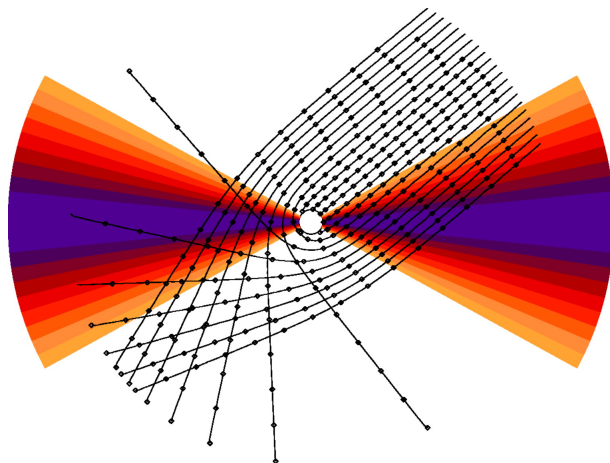


Figure 1. Schematic diagram of a typical ray-tracing procedure. The path of a photon is integrated along geodesic trajectories from a distant observer to the region close to the black hole. The photons may either terminate at the horizon (innermost circle) or escape to infinity. The source of photons in this example is an accretion disk with layers (in color) of different temperature. Figure taken from Reference [37] with kind permission from J. Schnittman and reproduced by permission of the AAS.

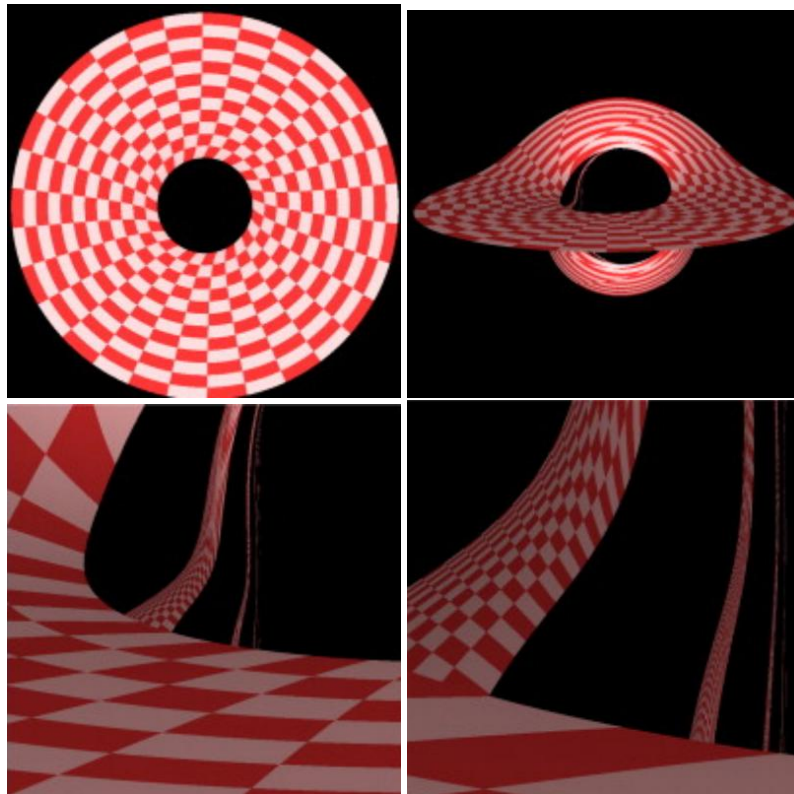


Figure 2. Ray-tracing of a thin accretion disk around an extreme Kerr black hole with mass $M = 1$ and Kerr parameter $a = 1$. The observer is located at a distance of $50 M$ at inclination angles of 2 deg (left) and 80 deg (three right panels) with respect to the normal disk. The inner and outer disk radii are $r_{\text{in}} = 3 M$ and $r_{\text{out}} = 15 M$. Higher-order images of the disk become visible within a field of view of 5 deg (second from right) and 1.5 deg (right). Figure reprinted from Reference [38] with permission from Elsevier.

The same principle also applies and is observationally confirmed for weaker gravitational fields. The famous historical example is the deflection of light by stars predicted by Einstein [39] and its confirmation observed during a solar eclipse [40]. A modern application is the observation of gravitational lensing [8,9] for a variety of sources. Examples are the discovery of planets by micro-lensing events in the Milky Way [41], the observation of multiple images of distant quasars [42], or the measure of shear and flexion in the large scale structure of the universe (see, e.g., [43]).

Apart from the general relativistic effects discussed above, special relativistic Doppler beaming for moving sources (a jet or a disk) plays an essential role for the observed signal. The blue-shifted signal is Doppler-boosted, thus brighter, while the red-shifted signal is de-boosted for the observer.

In addition to the pure ray-tracing of light rays through space-time, radiative transfer can be applied, dealing with absorption and emissivity along the path of light. This problem is substantially more complex than dealing with material opacities or scattering and can be solved in approximations. However, in general, material properties such as densities, temperatures, etc. as well as the light sources can be provided by either a kinematic prescription or by post-processing of dynamical data resulting from a (magneto-)hydrodynamic simulation [37,44–49] (see below).

3. Dynamics and Feedback—(Magneto-)Hydrodynamic Simulations

Black holes are able to feed back to their environment—implying that mass, energy or angular momentum is taken away from the accompanying components or the black hole itself and is deposited further away from the black hole.

A typical context is the nuclear activity of a galaxy, such as quasars with extremely high luminosity that arises from the black hole accretion disk, or radio galaxies that may drive Mpc-long relativistic jets. These feedback processes are thought to be essential for cosmological structure formation and the formation of galaxies [2]. On lower energy scales, similar processes work in Galactic micro-quasars that are powered by stellar-mass black holes [1]. In a similar way, central black holes are believed to be the very origin of the explosive Gamma-ray bursts observed on cosmological distances [50].

A fundamental question that can be tackled by a numerical treatment is the mass accretion to the black hole. The physics of the accretion process determines the black hole luminosity and also the growth of the black hole mass (and angular momentum). Quite a number of general relativistic simulations of black hole accretion flows have been carried out over the last few decades, both in the hydrodynamic limit (e.g., [12,14,15,51,52]), but also applying MHD, and some of them even considering some sort of radiative transport (e.g., [11,20,53–55]).

The physical origin of magnetized jet outflows has been proposed in seminal papers by the authors of [6,7]. The first mechanism—known as the Blandford–Znajek mechanism—works only for rotating black holes. Here, the frame dragging of space-time leads to the induction of a toroidal magnetic field from the poloidal magnetic field threading the black hole ergosphere. As a result, a strong Poynting flux can be generated, leading to a magnetically dominated jet tower that can be filled by lepton pairs that are produced by the strong radiation field of the accretion disk.

The second mechanism—known as the Blandford–Payne mechanism—deals with the acceleration and collimation of disk winds by magneto-centrifugal forces. Many nonrelativistic MHD simulations on this topic have been published (see, e.g., [56]), but also a few relativistic simulations that show that this effect may also work in relativity [57,58]. However, it seems to be difficult to gain very high Lorentz factors for disk winds [59].

The launching question—the question of how the disk wind material is lifted into the outflow—is more complex and requires treating the accretion disk evolution simultaneously. Analytical (nonrelativistic) theory has demonstrated that magnetic diffusivity (respectively, resistivity) is essential for launching [60]—that implies redistributing material between different magnetic flux surfaces and, by that, feeding the outflow with disk material.

Simulations of wind or jet launching from thick hot disks have been performed applying nonrelativistic codes [61,62], see also Yuan & Narayan [63]. Similarly, launching simulations of jets from thin disks have been published (see, for example, [64–66] pointing out again importance of the magnetic diffusivity for mass loading. From nonrelativistic simulations, we also know that disk magnetization plays a leading role for governing the outflow properties [67].

General relativistic MHD simulations were pioneered by the authors of [13], while the first results were published by the authors of [17]. Soon, further numerical codes became available boosting the number of publications in this field [11,16,19,20,23,24,68–72]. Over the last decade, constant and rapid progress in this field has been made.

Most often, for the simulation, a stationary hydrodynamic torus [73] is assumed as the initial condition from which a (thin) disk may emerge. However, it looks like some leading parameters of the flow evolution seem to be determined by this (probably not realistic) initial setup and are not “forgotten” during the simulation, so its use may be limited (see, e.g., [74]). The torus-disk structure evolves under magneto-rotational instability [28], leading to accretion of material towards the black hole and also to weak disk winds. Advection of magnetic flux along the disk towards the black hole leads to the accumulation of a strong axial poloidal flux that “threads” the black hole.

The feasibility of the so-called Blandford–Znajek mechanism was numerically demonstrated by the authors of [22] through pure electromagnetic simulations and later also by a number of MHD simulations in general relativity (see, for example, [20,21,69,70,75,76]).

Figure 3 shows the result from a 3D GR-MHD simulation investigating the stability of jets launched by a rotating black hole [77]. The authors found jets with a Lorentz factor of about 10 emerging along the black hole rotational axis with opening angles of about 10 degrees. The jet reaches about 1000

gravitational radii distance from the black hole without significant distortion by a 3D instability. These numbers are constrained by the numerical capability of the available codes. So far, much higher relativistic jets cannot be modeled, meaning that the jet mass fluxes and the jet speed are limited by the floor model (see above). Jet stability is essentially affected by the numerical resolution and also by the conditions in the environment.

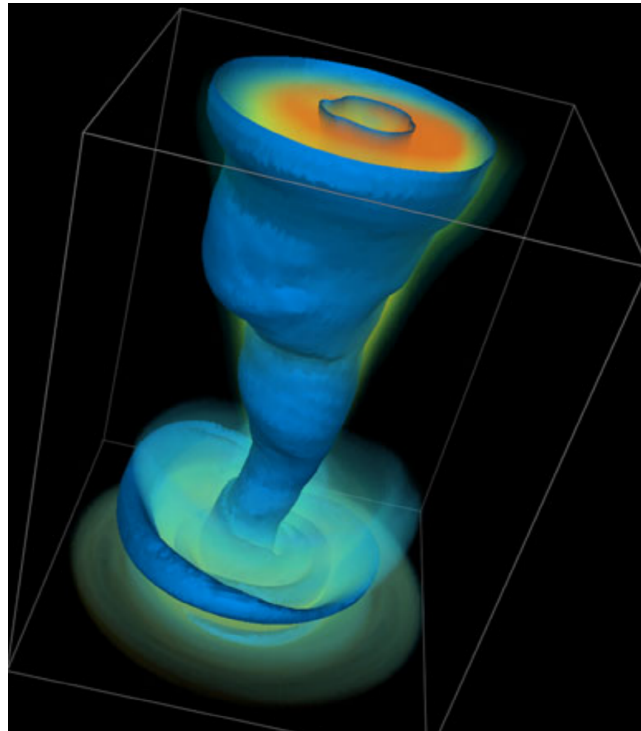


Figure 3. Jet launching simulation applying 3D GR-MHD. Shown is the volume rendering of the internal energy density (log scale) for the relativistic black hole jet within a box of $350 \times 350 \times 1000$ black hole gravitational radii R_g after $t = 4000$ time units $t_g = R_g/c$. Only the jet, not the counter jet, is shown, and fragments of the perturbed disk wind. The jet reaches Lorentz factors of $\Gamma \lesssim 10$ and a half-opening angle of $\Theta_{\text{jet}} \simeq 5^\circ$. Figure taken from Reference [77], with kind permission of J. McKinney and by permission of Oxford University Press on behalf of the Royal Astronomical Society.

Of particular interest is the so-called plunging region between the inner disk radius (located approximately at the innermost stable orbit, ISCO) and the horizon. Of course, the generation of jets driven by black hole rotation is also governed by this area. This region is, in particular, sensitive to the frame dragging of a spinning black hole and also determines the energy conversion from the potential and orbital energy of the disk material. Examples for simulations emphasizing on the plunging region are Reference [78], which investigated how the electromagnetic stresses within the ISCO depend on the black hole spin or the thickness of the accretion disk; or Reference [79], which considered jet formation in from magnetically arrested disks. In Reference [80], the interrelation between black hole spin and the jet power output apply their results to the long-standing problem of the radio loud/quiet dichotomy of AGN. In a similar approach, Reference [81] found that black holes that rotate prograde compared to the disk may trap more magnetic flux than retrograde black holes, leading to a higher jet efficiency.

The time-evolution of thin disks has been studied by the authors of [82], in particular considering the evolution of and the electromagnetic stress at the inner disk radius in the Schwarzschild case. This is important in order to understand the efficiency of the accretion process and the time scale for black hole growth. Tilted thin disks and the potential onset of precession due to the Bardeen–Petersen effect were investigated by the authors of [54] in 3D simulations lasting up to 13,000 time units $t_g = R_g/c$ that are measured in light crossing time over the gravitational radius R_g . Precession of the central

black hole or the inner accretion disk may be seen as a time-dependent alignment of the jet outflow on much larger (pc-kpc) scale.

Resistive GR-MHD have also been applied, in particular to investigate the magnetic field generation by a dynamo process [83,84], to compare the energy output from the disk wind and the Blandford–Znajek jet [85,86], or a stellar magnetized collapse to a black hole [87,88].

4. Radiation from Simulated Gas Dynamics

From GR-MHD simulations of the black hole environment, the time evolution of the gas dynamics and the magnetic field can be derived. However, what is observed in reality is the radiation that is emitted from this gas—observers obtain spectra or radiation images. In order to compare simulation results with observations, it is therefore essential to couple radiation transfer to the hydrodynamics of the simulation.

Most of the emission from the black hole source is expected to come from the innermost accretion disk. However, the light that is emitted in the plunging region during the final infall may actually carry most of potential (general) relativistic imprints, in particular imprints from the metric that is defined by the central black hole. By simulating these signals and comparing them to observations, we may gain direct information about the black hole characteristics, such as, e.g., the black hole spin (see, e.g., [89]).

Combining MHD dynamics and radiation transfer is computationally highly expensive and yet numerically and physically still limited. A number of issues have to be considered. The method of choice would be to do radiation transfer modeling along with the hydrodynamics, that is, to follow the absorption and emission of photons by the gas along with the gas dynamics.

It is well known that the radiation transfer equations need to be *closed*. A closure relation is needed as radiation transfer is typically treated considering *moments* such as radiation energy, radiation flux, and radiation pressure. The local geometry of the radiation field needs to be specified by a radiation model (for example, LTE), which closes the set of radiation transfer equations. A few astrophysical options for the closure problem have been established. Each method may have its advantages and disadvantages for a certain astrophysical problem. One option is the flux-limited diffusion, applied for a short mean free path of photons and thus, for large optical depth close to the case of LTE. The application of the diffusion approximation is often coarse; however, radiative transfer would be very expensive. A well known closure is the Eddington approximation, typically applied in a plane-parallel geometry like a geometrically thin stellar photosphere. However, this is probably not a good choice for a turbulent disk-jet structure around a black hole.

The method of choice applied in most GR-MHD simulations is the so-called M1 closure that evolves the radiation flux independently from the radiation energy. The basic assumption is that the radiation field is locally a dipole aligned with the radiation flux. The M1 closure has been introduced in GR hydrodynamics by the authors of [90] and for special relativistic magnetized fluids by the authors of [91]. In contrast to the diffusion limit, M1 could handle “shadows”. In Reference [55], this approach was applied to investigate the impact of opacity on the accretion flow structure and evolution in cases of super-Eddington luminosities. In a similar way, Reference [92] could model super-Eddington disks with accretion rates 100–200 times the Eddington accretion rate.

Another closure that was recently be proposed is the Monte–Carlo closure for general relativistic radiation hydrodynamics [93]. This was also applied in particular to investigate the neutrino transport. Neutrino transport has been proven to be essential for the understanding the neutrino emission they radiate along with the gravitational waves when forming a black hole [94].

A computationally less expensive approach that avoids the costly radiative transfer modeling is to consider a cooling function in the GR-MHD simulation. This method was introduced in GR-MHD by the authors of [11] to calculate the radiative efficiency of the black hole disk. The disk radiation was ray-traced to compute the flux that was eventually received by the observer. In Reference [95], the mm and sub-mm flux for Sgr A* was derived. Spectra and radiation maps were derived, applying

various combinations of the black hole spin parameter and the disk accretion rate in order to match the observed 1-mm flux of 4 Jy. In Reference [45], the authors compared the numerically derived disk luminosity to observations of Sgr A*, deriving an accretion rate of $5_{-2}^{+15} \times 10^{-9} M_{\odot} \text{ year}^{-1}$ as well as temperatures and inclination angle. Similarly, Reference [96] derived spectra from GR-MHD modeling and compared them to the properties of Sgr A*. In particular, they showed that by combining this information with the emission images, certain models (those with strong funnel emission) can be ruled out. Heating and cooling of electrons were included in recent GR-MHD simulations by the authors of [97,98].

A widely used approach to construct black hole radiation features is post-processing of the simulated MHD data. This is an option, for example, when considering the *nonthermal radiation* or optically thin cases. For nonthermal emission, however, the energy distribution of the emitting high energy particles cannot be derived self-consistently within the MHD approach and must thus be prescribed. Depending on whether the particle energies are interrelated with the gas pressure, the gas density or the magnetic field energy, the resulting radiation maps may vary greatly (see, e.g., [58]).

Post-processing of radiation features is always problematic when dealing with optically thick media. The optical depth of the material and also its opacity is not always known, and post-processing remains an approximation. This is in particular an issue when dealing with *thermal emission*. Then, ideally, radiation transport should be done along with the MHD simulation (as discussed above), as the radiation field may affect the gas temperature that in turn governs the radiation field.

We mention another issue for this method that is linked to the coordinate system and time stepping generally used by GR-MHD codes. GR-MHD simulations are typically performed in (modified) Kerr–Schild coordinates, thus providing time slices—snapshots—in Kerr–Schild time. Observations—ray tracing—are typically done in the observers’ frame, for example, in Boyer–Lindquist coordinates. The difficulty is that in every snapshot in Kerr–Schild coordinates—representing a 2D or 3D distribution of, e.g., gas density or magnetic field—each pixel represents a *different time* in Boyer–Lindquist coordinates. Thus, performing a ray-tracing along the photon path that is smooth in time seems impossible.

In addition to that, ray-tracing across material that moves relativistically needs to consider the *retarded times*. The problem is that while the signal (emitted at a certain retarded time) is propagating with time through the gas, “new” material is moving *into* that path of the photon (this motion is actually) calculated by the GR-MHD simulation. It is therefore difficult to interpret post-processed radiation maps for highly time-variable sources, such as jets or accretion disk coronae.

So far, ray tracing in GR-MHD-simulated gas dynamics circumvents this problem by assuming the so-called *fast-light approximation* that postulates that the light travels faster than the dynamics of the system evolves. Another option to get (post-processed) mock images of simulation data is to stack simulation snapshots and ray-trace along the time-averaged gas distribution. While this is a valid approach in order to obtain time-averaged radiation features such as a typical spectrum of the source, the method is obviously not applicable for highly time-variable phenomena.

In reality, post-processing of radiation transfer may not be fully consistent with the dynamics of the relativistic plasma, but at the moment, there seem to be no numerical tools at hand that can circumvent this problem in respect of the available CPU resources. Post-processing radiative transfer is widely applied [37,44–47,49,99–101] and has recently also been extended for comptonization [102].

As a specific example, we mention Reference [37], the authors of which derived light curves of black hole accretion disks from radiative transfer based on GR-MHD simulations with the application on quasi-periodic oscillations of X-ray binaries. In Reference [103], a comparison study of black hole shadow images for Sgr A* was presented, demonstrating the impact of, e.g., the inclination angle and the temperature prescription, scattering, or the stacking of images on the visibility of the shadow. This is shown in Figure 4, demonstrating the complexity of the parameter space and thus, the difficulty to obtain “true” radiation maps. The authors concluded that all these effects together *may* make it difficult to unambiguously detect the black hole shadow or to extract information about the space-time from its

size and shape, before the plasma physics and dynamical properties of disk and jet are constrained (see also [104]).

Nevertheless, mock observations from simulated MHD simulations of the black hole environment are extremely important for understanding the observations of the “shadow” of nearby supermassive black holes (Sgr A* and M87) as proposed by the Event Horizon Telescope (EHT) initiative (see <https://eventhorizontelescope.org/>). Radiation transfer modeling is essential in order to disentangle the various processes at work at these spatial scales, such as disk and outflow dynamics, light bending, or absorption or scattering [96,101].

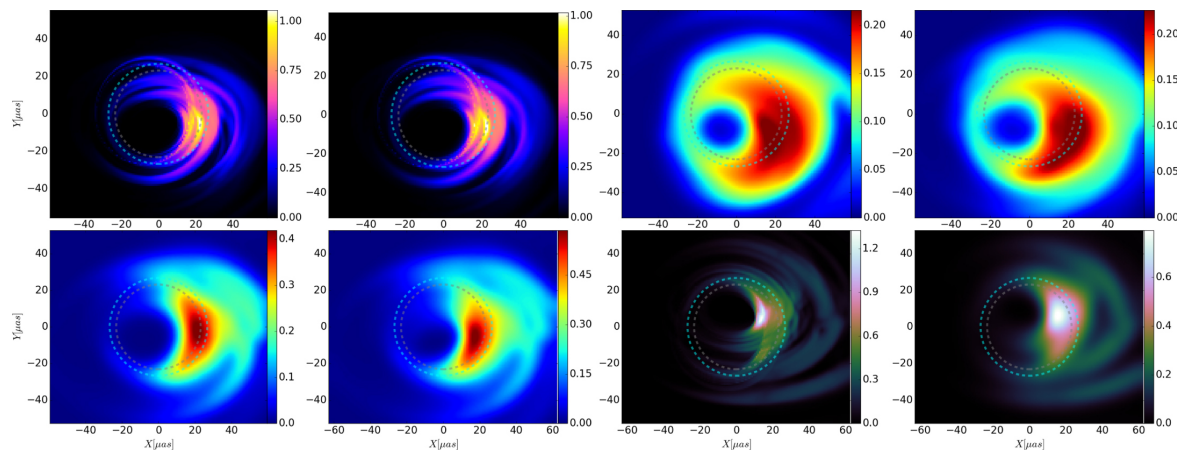


Figure 4. Black hole shadow image plane intensity plots for the Galactic center black hole Sgr A* as calculated from a model geometry consisting of a disk and jet around a black hole. The series demonstrates the richness in the parameter space that can be considered, such as (i) a single observer comparison to the parameter space of [45]; (ii) instead, eight snapshots time-averaged; (iii) applying an inclination of $i = 45^\circ$, and a fixed ion-to-electron temperature (as in Moscibrodzka et al. (2009)); (iv) applying another default time instead (little difference); (v) applying different jet and gas temperatures (no isothermal jet); (vi) applying an isothermal jet; (vii) a best-fit for all parameters; and (viii) also including scattering. Figure taken from Reference [103] with kind permission from R. Gold and reproduced by permission of the AAS.

5. Compact Object Mergers

“For a brief moment, a binary black hole merger can be the most powerful astrophysical event in the visible Universe” [105]. The numerical treatment of compact object mergers is considerably the most difficult numerical task to date. While the dynamical evolution of the material around a single black hole can be treated on a fixed space-time, the evolution of (close) binary black holes is substantially more complex. As the metric changes with time, for this problem, the Einstein equations need to be solved numerically in a way that (i) allows for a well-posed initial-boundary-value problem, and that (ii) singularities inherent in the black hole space-times can be circumvented (see, e.g., [106,107]). The same challenges appear for mergers of binary neutron stars into a black hole.

In comparison to the simulations discussed in the last sections, most simulations of black hole mergers typically consider only gravity. Therefore, the results depend only on a few parameters (black hole masses and spins) and do not rely on further assumptions on physical quantities, such as, e.g., the accretion disk density or the magnetic field. Fundamental breakthrough in the simulation of binary black holes came around 2005 with seminal papers considering the three basic phases of a black hole merger—the orbit (only up to a single orbit in these early years), the merger, and the following ringdown [108–111].

Deriving the gravitational wave signal from a merger in its final stage requires evolving the 3D Einstein equations. Further, the merger simulation has to run sufficiently long [112,113]. An early example of the gravitational wave signal and the apparent horizons of the merging black hole as

derived by the authors of [108] is shown in Figure 5. These early modeling efforts succeeded through using excision in excluding singular regions within the horizons (see above). For the extraction of the wave signal from the numerical simulation of the merger—thus extracting the radiative part of the numerical solution of the Einstein equations—a number of methods have been developed. For a detailed discussion of the problems involved, we refer to Reference [114].

The field of compact merger simulations has evolved rapidly, also benefiting from the advance in CPU power. Some codes, such as the “Einstein Toolkit”, have even been made publicly available [115,116]. Hundreds of binary black hole simulations have been performed by now, allowing to do proper statistics of gravitational wave forms and the gravitational wave luminosity or on the final black hole properties based on different initial mass ratios or black hole spins (see, e.g., [105,117,118]). A recent, colorful 3D representation of the merging black holes emitting gravitational waves is shown in Figure 6.

As it is considerably one of the most fascinating events in recent science, the long lasting efforts in both theoretical predictions and detector experiments culminated in 2015 when the LIGO interferometer eventually detected a gravitational wave signal [119,120] that was perfectly matching the theoretically predicted waveform models for a black hole merger [121,122]. The detection clearly indicates a black hole merger of masses of $36_{-4}^{+5}M_{\odot}$ and $29_{-4}^{+4}M_{\odot}$ to a final black hole of mass $62_{-4}^{+4}M_{\odot}$ at a luminosity distance of 410_{-180}^{+160} Mpc, thereby radiating away gravitational waves ¹ of energy of $3.0_{-0.5}^{+0.5}M_{\odot}c^2$. In addition to the fascinating confirmation of the existence of gravitational waves, the data also revealed a new and unexpected mass range for black holes. As of early 2019, gravitational wave detections have reached the number of 11 (for the actual status, see <https://www.ligo.caltech.edu/page/detection-companion-papers>).

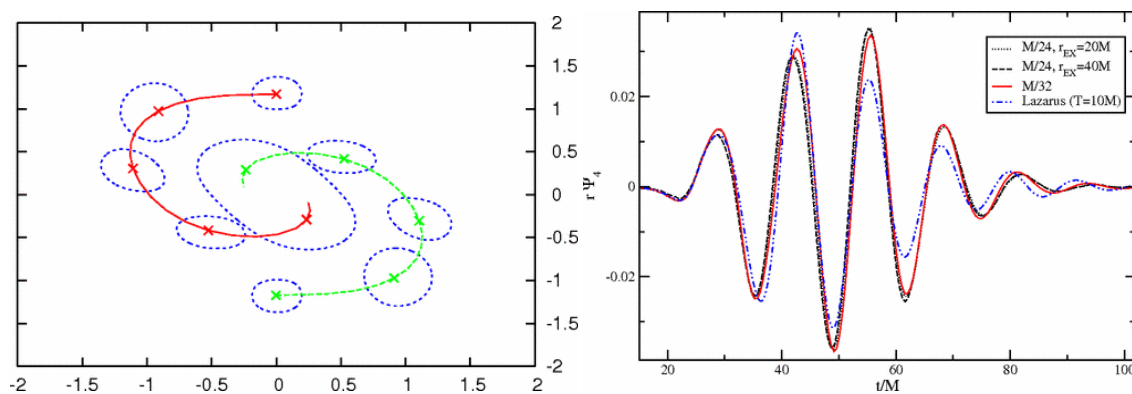


Figure 5. Early example of a merging binary black hole simulation. Positions of the apparent horizons (left) with time, $t = 0, 5, 10, 15,$ and $20 M$. The line shows the trajectories of centroids of the individual apparent horizons (dashed). Gravitational wave signal (right) for simulation runs of different resolution. Figures reprinted from Reference [108] (doi:10.1103/PhysRevLett.96.111102) with kind permission of J.G. Baker, and the American Physical Society (copyright 2006).

Another class of merger simulations consider mergers of neutron star binaries. This field was pioneered by Shibata and Uryu [123–125]. Binary neutron star mergers are related to black hole numerics, as these mergers *do form* a black hole. As a matter of fact, these kind of mergers may provide an observational signal in addition to the pure gravitational wave.

A particular difficulty in neutron star merger simulations compared to black hole merger simulations is that one has to consider *material* with a certain equation of state. However, despite a

¹ Interested readers can actually redo the modeling of the GW 150914 binary black hole merger gravitational wave signal using the “Einstein Toolkit”, see <https://einstein toolkit.org/gallery/bbh/>.

huge observational and theoretical progress, the equation of state for neutron stars is still one of the major unsolved problems in astrophysics (see, e.g., [126,127]).

Merger simulations investigating different nuclear equations of state have been performed [128], indicating, for example, that different kinds of final merger states can be realized that are strongly dependent on the equation of state applied. Simulations of this kind also allow tackling the evolution of a massive torus surrounding the remnant black hole. In turn, the gravitational wave signal from binary neutron star mergers could be used to probe the extreme-density matter in these stars [129].

Examples for further specifics of neutron star mergers in comparison to black hole merges are tidal effects of the stellar mass distribution [130], a possible mass ejection and radiation [131], or neutrino emission [94]. Further, neutron star mergers have long been discussed as sources of short gamma-ray bursts; therefore, simulations of such a scenario are essential to confirm this hypothesis [132,133]. A particularly exciting example of this kind of simulations is the modeling [134] of the gravitational wave signal GW170817 that was connected to the simultaneous detection of a gamma ray burst [135].

A remaining step would be the combination of the two approaches discussed above, namely, the combination of a merger simulation with the magneto-hydrodynamics of the binary black hole environment, thus combining the numerical approach discussed in this section (pure gravity) with the dynamical MHD simulations discussed before. This has been achieved by, e.g., the authors of [136], who, for the first time, ran fully general relativistic MHD simulations of an equal-mass black-hole binary merger in a magnetized, circum-(black hole)-binary accretion disk (see also [137]). Such simulations can predict, for example, the change of accretion rate during the merger event. Essentially, they may also provide—in addition to the binary merger gravitational wave signal—the contemporary electromagnetic signal during the merger event.

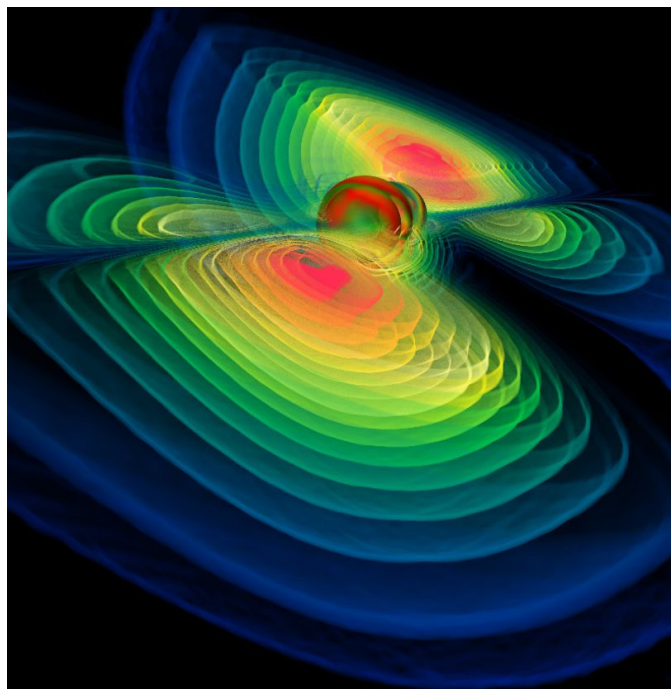


Figure 6. A numerical simulation showing the gravitational radiation emitted by the violent merger of two black holes. Figure taken from Reference [138] with kind permission from B. Brügmann; Credits: Visualisation by Werner Benger, Albert Einstein Institute, Max Planck Institute of Gravitational Physics, Potsdam, Germany.

6. Summary and Outlook

This brief (and therefore incomplete) review intended to summarize the rapid development and the various applications of numerical methods in general relativity over the past decades.

The numerical approaches involving black holes can roughly be distinguished in simulations (i) treating the dynamics of the black hole environment on a fixed metric; or (ii) solving for time-dependent solutions of the Einstein equations that allow following the merger of compact objects into a remnant black hole and the gravitational waves that are emitted; or (iii) following the photons that are affected by strong gravity, and thus allowing to see how black holes “look alike”. Even more demanding are combinations of these approaches, such as obtaining mock observations of simulated dynamical data involving magneto-hydrodynamics and radiation transfer.

The comfortable situation today is that quite a number of codes have been developed for these different approaches. In addition, the computational resources to operate them have also vastly improved. An essential point is comparing the existing codes and the robustness of their results concerning, e.g., the accretion towards the black hole. This task is currently undertaken as a collaboration of nine groups and the first results are published recently [139].

In addition to fundamental questions of theoretical physics, such as testing general relativity in the strong field limit, from an astrophysical perspective, the most intriguing problems are maybe (i) the formation and early growth of (distant) supermassive black holes—most cases probably involving both the merger scenario and disk accretion; (ii) the mystery of gamma-ray bursts; or (iii) the inner structure (the equation of state) and the evolution of compact stars.

Essential observational input is expected from future gravitational wave signals measured by LIGO, as well as from highly resolved radio observations that are going to image the shadow of nearby supermassive black holes. Striking first images of a black hole shadow, namely that of the nearby galaxy M87 and corresponding simulations in GR-MHD, which are essential for the interpretation of the data, have been published by the EHT collaboration very recently [140,141].

With all the advances in the observational data that will become available, numerical modeling will be central to the understanding of these findings.

Funding: This research received no external funding.

Conflicts of Interest: The author declares no conflict of interest.

Abbreviations

The following abbreviations are used in this manuscript:

3D	Three-dimensional
AGN	Active galactic nuclei
EHT	Event Horizon Telescope
GR-MHD	General relativistic magneto-hydrodynamics
ISCO	Innermost stable circular orbit
LIGO	Laser Interferometer Gravitational-Wave Observatory
MHD	Magneto-hydrodynamics

References

1. Mirabel, I.F.; Rodríguez, L.F. Sources of Relativistic Jets in the Galaxy. *Ann. Rev. Astron. Astrophys.* **1999**, *37*, 409–443.
2. Fabian, A.C. Observational Evidence of Active Galactic Nuclei Feedback. *Ann. Rev. Astron. Astrophys.* **2012**, *50*, 455–489.
3. Netzer, H. *The Physics and Evolution of Active Galactic Nuclei*; Cambridge University Press: Cambridge, UK, 2013.
4. Shakura, N.I.; Sunyaev, R.A. Black holes in binary systems. Observational appearance. *Astron. Astrophys.* **1973**, *24*, 337–355.
5. Blandford, R.D.; McKee, C.F. Reverberation mapping of the emission line regions of Seyfert galaxies and quasars. *Astrophys. J.* **1982**, *255*, 419–439.

6. Blandford, R.D.; Payne, D.G. Hydromagnetic flows from accretion discs and the production of radio jets. *Mon. Not. R. Astron. Soc.* **1982**, *199*, 883–903.
7. Blandford, R.D.; Znajek, R.L. Electromagnetic extraction of energy from Kerr black holes. *Mon. Not. R. Astron. Soc.* **1977**, *179*, 433–456. [[CrossRef](#)]
8. Einstein, A. Lens-Like Action of a Star by the Deviation of Light in the Gravitational Field. *Science* **1936**, *84*, 506–507. [[CrossRef](#)] [[PubMed](#)]
9. Refsdal, S. The gravitational lens effect. *Mon. Not. R. Astron. Soc.* **1964**, *128*, 295–306. [[CrossRef](#)]
10. Jiang, Y.-F.; Davis, S.W.; Stone, J.M. Iron Opacity Bump Changes the Stability and Structure of Accretion Disks in Active Galactic Nuclei. *Astrophys. J.* **2016**, *827*, 10. [[CrossRef](#)]
11. Noble, S.C.; Krolik, J.H.; Hawley, J.F. Direct Calculation of the Radiative Efficiency of an Accretion Disk Around a Black Hole. *Astrophys. J.* **2009**, *692*, 411.
12. Wilson, J.R. Numerical Study of Fluid Flow in a Kerr Space. *Astrophys. J.* **1972**, *173*, 431. [[CrossRef](#)]
13. Wilson, J.R. Magnetohydrodynamics near a black hole. In *Proceedings of the Marcel Grossman Meeting*; North Holland: Amsterdam, The Netherlands, 1977.
14. Hawley, J.F.; Smarr, L.L.; Wilson, J.R. A numerical study of nonspherical black hole accretion. I Equations and test problems. *Astrophys. J.* **1984**, *277*, 296. [[CrossRef](#)]
15. Hawley, J.F.; Smarr, L.L.; Wilson, J.R. A numerical study of nonspherical black hole accretion. II—Finite differencing and code calibration. *Astrophys. J. Suppl. Ser.* **1984**, *55*, 211–246. [[CrossRef](#)]
16. De Villiers, J.-P.; Hawley, J.F. Three-dimensional Hydrodynamic Simulations of Accretion Tori in Kerr Spacetimes. *Astrophys. J.* **2002**, *577*, 866. [[CrossRef](#)]
17. Koide, S.; Shibata, K.; Kudoh, T. Relativistic Jet Formation from Black Hole Magnetized Accretion Disks: Method, Tests, and Applications of a General Relativistic Magnetohydrodynamic Numerical Code. *Astrophys. J.* **1999**, *522*, 727. [[CrossRef](#)]
18. Del Zanna, L.; Zanotti, O.; Bucciantini, N.; Londrillo, P. ECHO: A Eulerian conservative high-order scheme for general relativistic magnetohydrodynamics and magnetodynamics. *Astron. Astrophys.* **2007**, *473*, 11. [[CrossRef](#)]
19. De Villiers, J.-P.; Hawley, J.F. A Numerical Method for General Relativistic Magnetohydrodynamics. *Astrophys. J.* **2003**, *589*, 458. [[CrossRef](#)]
20. Gammie, C.F.; McKinney, J.C.; Tóth, G. HARM: A Numerical Scheme for General Relativistic Magnetohydrodynamics. *Astrophys. J.* **2003**, *589*, 444. [[CrossRef](#)]
21. Koide, S. Magnetic extraction of black hole rotational energy: Method and results of general relativistic magnetohydrodynamic simulations in Kerr space-time. *Phys. Rev. D* **2003**, *67*, 104010. [[CrossRef](#)]
22. Komissarov, S.S. Direct numerical simulations of the Blandford-Znajek effect. *Mon. Not. R. Astron. Soc.* **2001**, *326*, L41 [[CrossRef](#)]
23. McKinney, J.C. General relativistic force-free electrodynamics: A new code and applications to black hole magnetospheres. *Mon. Not. R. Astron. Soc.* **2006**, *367*, 1797. [[CrossRef](#)]
24. Noble, S.C.; Gammie, C.F.; McKinney, J.C.; Del Zanna, L. Primitive Variable Solvers for Conservative General Relativistic Magnetohydrodynamics. *Astrophys. J.* **2006**, *641*, 626. [[CrossRef](#)]
25. Denicol, G.S.; Kodama, T.; Koide, T.; Mota, P. Stability and causality in relativistic dissipative hydrodynamics. *J. Phys. G Nuclear Phys.* **2008**, *35*, 115102. [[CrossRef](#)]
26. Hiscock, W.A.; Lindblom, L. Stability and causality in dissipative relativistic fluids. *Ann. Phys.* **1983**, *151*, 466 [[CrossRef](#)]
27. McKinney, J.C.; Narayan, R. Disc-jet coupling in black hole accretion systems—II. Force-free electrodynamic models. *Mon. Not. R. Astron. Soc.* **2007**, *375*, 531. [[CrossRef](#)]
28. Balbus, S.A.; Hawley, J.F. A powerful local shear instability in weakly magnetized disks. I—Linear analysis. *Astrophys. J.* **1991**, *376*, 214. [[CrossRef](#)]
29. Smarr, L. Mass Formula for Kerr Black Holes. *Phys. Rev. Lett.* **1973**, *30*, 71. [[CrossRef](#)]
30. Smarr, L.; Cadez, A.; Dewitt, B.; Eppley, K. Collision of two black holes: Theoretical framework. *Phys. Rev. D* **1976**, *14*, 2443. [[CrossRef](#)]
31. Smarr, L.; York, J.W., Jr. Kinematical conditions in the construction of spacetime. *Phys. Rev. D* **1978**, *17*, 2529. [[CrossRef](#)]
32. Eardley, D.M.; Smarr, L. Time functions in numerical relativity: Marginally bound dust collapse. *Phys. Rev. D* **1979**, *19*, 2239. [[CrossRef](#)]

33. Anninos, P.; Massó, J.; Seidel, E.; Suen, W.-M.; Towns, J. Three-dimensional numerical relativity: The evolution of black holes. *Phys. Rev. D* **1995**, *52*, 2059. [[CrossRef](#)]
34. Brandt, S.R.; Seidel, E. Evolution of distorted rotating black holes. III. Initial data. *Phys. Rev. D* **1996**, *54*, 1403. [[CrossRef](#)]
35. Varma, V.; Scheel, M.A.; Pfeiffer, H.P. Comparison of binary black hole initial data sets. *Phys. Rev. D* **2018**, *98*, 104011. [[CrossRef](#)]
36. Cook, G.B.; Huq, M.F.; Klasky, S.A.; Klasky, S.A.; Scheel, M.A.; Abrahams, A.M.; Anderson, A.; Anninos, P.; Baumgarte, T.W.; Bishop, N.T.; et al. Boosted Three-Dimensional Black-Hole Evolutions with Singularity Excision. *Phys. Rev. Lett.* **1998**, *80*, 2512. [[CrossRef](#)]
37. Schnittman, J.D.; Krolik, J.H.; Hawley, J.F. Light Curves from an MHD Simulation of a Black Hole Accretion Disk. *Astrophys. J.* **2006**, *651*, 1031. [[CrossRef](#)]
38. Müller, T. GeoVis-Relativistic ray tracing in four-dimensional spacetimes. *Comput. Phys. Commun.* **2014**, *185*, 2301. [[CrossRef](#)]
39. Einstein, A. Über den Einfluß der Schwerkraft auf die Ausbreitung des Lichtes. *Ann. Phys.* **1911**, *340*, 898. [[CrossRef](#)]
40. Dyson, F.W.; Eddington, A.S.; Davidson, C. A Determination of the Deflection of Light by the Sun's Gravitational Field, from Observations Made at the Total Eclipse of May 29, 1919. *Philos. Trans. R. Soc. Lond.* **1920**, *220*, 291–333. [[CrossRef](#)]
41. Beaulieu, J.-P.; Bennett, D.P.; Fouqué, P. Discovery of a cool planet of 5.5 Earth masses through gravitational microlensing. *Nature* **2006**, *439*, 437. [[CrossRef](#)]
42. Huchra, J.; Gorenstein, M.; Kent, S.; Shapiro, I.; Smith, G.; Horine, E.; Perley, R. 2237 + 0305: A new and unusual gravitational lens. *Astron. J.* **1985**, *90*, 691–696. [[CrossRef](#)]
43. Blandford, R.D.; Narayan, R. Cosmological applications of gravitational lensing. *Ann. Rev. Astron. Astrophys.* **1992**, *30*, 311. [[CrossRef](#)]
44. Chan, C.-K.; Psaltis, D.; Özel, F. GRay: A Massively Parallel GPU-based Code for Ray Tracing in Relativistic Spacetimes. *Astrophys. J.* **2013**, *777*, 13. [[CrossRef](#)]
45. Dexter, J.; Agol, E.; Fragile, P.C.; McKinney, J.C. The Submillimeter Bump in Sgr A* from Relativistic MHD Simulations. *Astrophys. J.* **2010**, *717*, 1092. [[CrossRef](#)]
46. Dexter, J. A public code for general relativistic, polarised radiative transfer around spinning black holes. *Mon. Not. R. Astron. Soc.* **2016**, *462*, 115. [[CrossRef](#)]
47. Pu, H.-Y.; Yun, K.; Younsi, Z.; Yoon, S.-J. Odyssey: A Public GPU-based Code for General Relativistic Radiative Transfer in Kerr Spacetime. *Astrophys. J.* **2016**, *820*, 105. [[CrossRef](#)]
48. Vincent, F.H.; Paumard, T.; Gourgoulhon, E.; Perrin, G. GYOTO: A new general relativistic ray-tracing code. *Class. Quant. Gravity* **2011**, *28*, 225011. [[CrossRef](#)]
49. Zhu, Y.; Narayan, R.; Sadowski, A.; Psaltis, D. HERO—A 3D general relativistic radiative post-processor for accretion discs around black holes. *Mon. Not. R. Astron. Soc.* **2015**, *451*, 1661. [[CrossRef](#)]
50. Kumar, P.; Zhang, B. The physics of gamma-ray bursts & relativistic jets. *Phys. Rep.* **2015**, *561*, 1.
51. Fragile, P.C.; Anninos, P. Hydrodynamic Simulations of Tilted Thick-Disk Accretion onto a Kerr Black Hole. *Astrophys. J.* **2005**, *623*, 347. [[CrossRef](#)]
52. Hawley, J.F. Three-dimensional simulations of black hole tori. *Astrophys. J.* **1991**, *381*, 496. [[CrossRef](#)]
53. Fragile, P.C.; Blaes, O.M.; Anninos, P.; Salmonson, J.D. Global General Relativistic Magnetohydrodynamic Simulation of a Tilted Black Hole Accretion Disk. *Astrophys. J.* **2007**, *668*, 417. [[CrossRef](#)]
54. Morales Teixeira, D.; Fragile, P.C.; Zhuravlev, V.V.; Ivanov, P.B. Conservative GRMHD Simulations of Moderately Thin, Tilted Accretion Disks. *Astrophys. J.* **2014**, *796*, 103. [[CrossRef](#)]
55. Sadowski, A.; Narayan, R.; McKinney, J.C.; Tchekhovskoy, A. Numerical simulations of super-critical black hole accretion flows in general relativity. *Astrophys. J.* **2014**, *439*, 503. [[CrossRef](#)]
56. Ouyed, R.; Pudritz, R.E. Numerical Simulations of Astrophysical Jets from Keplerian Disks. I. Stationary Models. *Astrophys. J.* **1997**, *482*, 712. [[CrossRef](#)]
57. Porth, O.; Fendt, C. Acceleration and Collimation of Relativistic Magnetohydrodynamic Disk Winds. *Astrophys. J.* **2010**, *709*, 1100. [[CrossRef](#)]
58. Porth, O.; Fendt, C.; Meliani, Z.; Vaidya, B. Synchrotron Radiation of Self-collimating Relativistic Magnetohydrodynamic Jets. *Astrophys. J.* **2011**, *737*, 42. [[CrossRef](#)]

59. Komissarov, S.S.; Vlahakis, N.; Königl, A.; Barkov, M.V. Magnetic acceleration of ultrarelativistic jets in gamma-ray burst sources. *Mon. Not. R. Astron. Soc.* **2009**, *394*, 1182–1212. [[CrossRef](#)]
60. Ferreira, J. Magnetically-driven jets from Keplerian accretion discs. *Astron. Astrophys.* **1997**, *319*, 340.
61. Yuan, F.; Bu, D.; Wu, M. Numerical Simulation of Hot Accretion Flows. II. Nature, Origin, and Properties of Outflows and their Possible Observational Applications. *Astrophys. J.* **2012**, *761*, 130. [[CrossRef](#)]
62. Yuan, F.; Gan, Z.; Narayan, R.; Sadowski, A.; Bu, D.; Bai, X. Numerical Simulation of Hot Accretion Flows. III. Revisiting Wind Properties Using the Trajectory Approach. *Astrophys. J.* **2015**, *084*, 101. [[CrossRef](#)]
63. Yuan, F.; Narayan, R. Hot Accretion Flows Around Black Holes. *Annu. Rev. Astron. Astrophys.* **2014**, *52*, 529 [[CrossRef](#)]
64. Zhu, Z.; Stone, J.M. Global Evolution of an Accretion Disk with a Net Vertical Field: Coronal Accretion, Flux Transport, and Disk Winds. *Astrophys. J.* **2018**, *857*, 34. [[CrossRef](#)]
65. Zanni, C.; Ferrari, A.; Rosner, R.; Bodo, G.; Massaglia, S. MHD simulations of jet acceleration from Keplerian accretion disks. The effects of disk resistivity. *Astron. Astrophys.* **2007**, *469*, 811. [[CrossRef](#)]
66. Sheikhezami, S.; Fendt, C.; Porth, O.; Vaidya, B.; Ghanbari, J. Bipolar Jets Launched from Magnetically Diffusive Accretion Disks. I. Ejection Efficiency versus Field Strength and Diffusivity. *Astrophys. J.* **2012**, *757*, 65. [[CrossRef](#)]
67. Stepanovs, D.; Fendt, C. An Extensive Numerical Survey of the Correlation Between Outflow Dynamics and Accretion Disk Magnetization. *Astrophys. J.* **2016**, *825*, 14. [[CrossRef](#)]
68. De Villiers, J.-P.; Hawley, J.F. Global General Relativistic Magnetohydrodynamic Simulations of Accretion Tori. *Astrophys. J.* **2003**, *592*, 1060. [[CrossRef](#)]
69. De Villiers, J.-P.; Hawley, J.F.; Krolik, J.; Hirose, S. Magnetically Driven Accretion in the Kerr Metric. III. Unbound Outflows. *Astrophys. J.* **2005**, *620*, 878. [[CrossRef](#)]
70. McKinney, J.C.; Gammie, C.F. A Measurement of the Electromagnetic Luminosity of a Kerr Black Hole. *Astrophys. J.* **2004**, *611*, 977. [[CrossRef](#)]
71. Narayan, R.; Sadowski, A.; Penna, R.F.; Kulkarni, A.K. GRMHD simulations of magnetized advection-dominated accretion on a non-spinning black hole: Role of outflows. *Mon. Not. R. Astron. Soc.* **2012**, *426*, 3241. [[CrossRef](#)]
72. Porth, O.; Olivares, H.; Mizuno, Y.; Younsi, Z.; Rezzolla, L.; Moscibrodzka, M.; Falcke, H.; Kramer, M. The black hole accretion code. *Comput. Astrophys. Cosmol.* **2017**, *4*, 1. [[CrossRef](#)]
73. Fishbone, L.G.; Moncrief, V. Relativistic fluid disks in orbit around Kerr black holes. *Astrophys. J.* **1976**, *207*, 962. [[CrossRef](#)]
74. Penna, R.F.; Kulkarni, A.; Narayan, R. A new equilibrium torus solution and GRMHD initial conditions. *Astron. Astrophys.* **2013**, *559*, A116. [[CrossRef](#)]
75. Komissarov, S.S. Observations of the Blandford-Znajek process and the magnetohydrodynamic Penrose process in computer simulations of black hole magnetospheres. *Mon. Not. R. Astron. Soc.* **2005**, *359*, 801. [[CrossRef](#)]
76. McKinney, J.C. Total and Jet Blandford-Znajek Power in the Presence of an Accretion Disk. *Astrophys. J.* **2005**, *630*, 5L. [[CrossRef](#)]
77. McKinney, J.C.; Blandford, R.D. Stability of relativistic jets from rotating, accreting black holes via fully three-dimensional magnetohydrodynamic simulations. *Mon. Not. R. Astron. Soc.* **2009**, *394*, L126. [[CrossRef](#)]
78. Penna, R.F.; McKinney, J.C.; Narayan, R.; Tchekhovskoy, A.; Shafee, R.; McClintock, J.E. Simulations of magnetized discs around black holes: effects of black hole spin, disc thickness and magnetic field geometry. *Mon. Not. R. Astron. Soc.* **2010**, *408*, 752. [[CrossRef](#)]
79. Tchekhovskoy, A.; Narayan, R.; McKinney, J.C. Efficient generation of jets from magnetically arrested accretion on a rapidly spinning black hole. *Mon. Not. R. Astron. Soc.* **2011**, *418*, L79. [[CrossRef](#)]
80. Tchekhovskoy, A.; Narayan, R.; McKinney, J.C. Black Hole Spin and The Radio Loud/Quiet Dichotomy of Active Galactic Nuclei. *Astrophys. J.* **2010**, *711*, 50. [[CrossRef](#)]
81. Tchekhovskoy, A.; McKinney, J.C. Prograde and retrograde black holes: whose jet is more powerful?. *Mon. Not. R. Astron. Soc.* **2012**, *423*, L55. [[CrossRef](#)]
82. Noble, S.C.; Krolik, J.H.; Hawley, J.F. Dependence of Inner Accretion Disk Stress on Parameters: The Schwarzschild Case. *Astrophys. J.* **2010**, *711*, 959. [[CrossRef](#)]
83. Bucciantini, N.; Del Zanna, L. A fully covariant mean-field dynamo closure for numerical 3 + 1 resistive GRMHD. *Mon. Not. R. Astron. Soc.* **2013**, *428*, 71. [[CrossRef](#)]

84. Bugli, M.; Del Zanna, L.; Bucciantini, N. Dynamo action in thick discs around Kerr black holes: high-order resistive GRMHD simulations. *Mon. Not. R. Astron. Soc.* **2014**, *440*, 41. [[CrossRef](#)]
85. Qian, Q.; Fendt, C.; Noble, S.; Bugli, M. rHARM: Accretion and Ejection in Resistive GR-MHD. *Astrophys. J.* **2017**, *834*, 29. [[CrossRef](#)]
86. Qian, Q.; Fendt, C.; Vourellis, C. Jet Launching in Resistive GR-MHD Black Hole—Accretion Disk Systems. *Astrophys. J.* **2018**, *859*, 28. [[CrossRef](#)]
87. Dionysopoulou, K.; Alic, D.; Palenzuela, C.; Rezzolla, L.; Giacomazzo, B. General-relativistic resistive magnetohydrodynamics in three dimensions: Formulation and tests. *Phys. Rev. D* **2013**, *88*, 044020. [[CrossRef](#)]
88. Palenzuela, C.; Lehner, L.; Reula, O.; Rezzolla, L. Beyond ideal MHD: Towards a more realistic modelling of relativistic astrophysical plasmas. *Mon. Not. R. Astron. Soc.* **2009**, *394*, 1727. [[CrossRef](#)]
89. Zhu, Y.; Davis, S.W.; Narayan, R.; Kulkarni, A.K.; Penna, R.F.; McClintock, J.E. The eye of the storm: Light from the inner plunging region of black hole accretion discs. *Mon. Not. R. Astron. Soc.* **2012**, *424*, 2504. [[CrossRef](#)]
90. Sadowski, A.; Narayan, R.; Tchekhovskoy, A.; Zhu, Y. Semi-implicit scheme for treating radiation under M1 closure in general relativistic conservative fluid dynamics codes. *Mon. Not. R. Astron. Soc.* **2013**, *429*, 3533. [[CrossRef](#)]
91. Takahashi, H.R.; Ohsuga, K. A Numerical Treatment of Anisotropic Radiation Fields Coupled with Relativistic Resistive Magnetofluids. *Astrophys. J.* **2013**, *772*, 127. [[CrossRef](#)]
92. McKinney, J.C.; Tchekhovskoy, A.; Sadowski, A.; Narayan, R. Three-dimensional general relativistic radiation magnetohydrodynamical simulation of super-Eddington accretion using a new code HARMRAD with M1 closure. *Mon. Not. R. Astron. Soc.* **2014**, *441*, 3177. [[CrossRef](#)]
93. Foucart, F. Monte Carlo closure for moment-based transport schemes in general relativistic radiation hydrodynamic simulations. *Mon. Not. R. Astron. Soc.* **2018**, *475*, 4186. [[CrossRef](#)]
94. Foucart, F.; Haas, R.; Duez, M.D.; O'Connor, E.; Ott, C.D.; Roberts, L.; Kidder, L.E.; Lippuner, J.; Pfeiffer, H.P.; Scheel, M.A. Low mass binary neutron star mergers: Gravitational waves and neutrino emission. *Phys. Rev. D* **2016**, *93*, 044019. [[CrossRef](#)]
95. Noble, S.C.; Leung, P.K.; Gammie, C.F.; Book, L.G. Simulating the emission and outflows from accretion discs. *Class. Quantum Gravity* **2007**, *24*, 5259. [[CrossRef](#)]
96. Chan, C.-K.; Psaltis, D.; Özel, F.; Narayan, R.; Sadowski, A. The Power of Imaging: Constraining the Plasma Properties of GRMHD Simulations using EHT Observations of Sgr A*. *Astrophys. J.* **2015**, *799*, 1. [[CrossRef](#)]
97. Ressler, S.M.; Tchekhovskoy, A.; Quataert, E.; Chandra, M.; Gammie, C.F. Electron thermodynamics in GRMHD simulations of low-luminosity black hole accretion. *Mon. Not. R. Astron. Soc.* **2015**, *454*, 1848. [[CrossRef](#)]
98. Ryan, B.R.; Ressler, S.M.; Dolence, J.C.; Tchekhovskoy, A.; Gammie, C.; Quataert, E. The Radiative Efficiency and Spectra of Slowly Accreting Black Holes from Two-temperature GRRMHD Simulations. *Astrophys. J.* **2017**, *844*, 24L. [[CrossRef](#)]
99. Dolence, J.C.; Gammie, C.F.; Moscibrodzka, M.; Leung, P.K. Grmonty: A Monte Carlo Code for Relativistic Radiative Transport. *Astrophys. J. Suppl. Ser.* **2009**, *184*, 387. [[CrossRef](#)]
100. Pu, H.-Y.; Akiyama, K.; Asada, K. The Effects of Accretion Flow Dynamics on the Black Hole Shadow of Sagittarius A*. *Astrophys. J.* **2015**, *831*, 4. [[CrossRef](#)]
101. Pu, H.-Y.; Wu, K.; Younsi, Z.; Asada, K.; Mizuno, Y.; Nakamura, M. Observable Emission Features of Black Hole GRMHD Jets on Event Horizon Scales. *Astrophys. J.* **2017**, *845*, 160. [[CrossRef](#)]
102. Narayan, R.; Zhu, Y.; Psaltis, D.; Sadowski, A. HEROIC: 3D general relativistic radiative post-processor with comptonization for black hole accretion discs. *Mon. Not. R. Astron. Soc.* **2016**, *457*, 608. [[CrossRef](#)]
103. Gold, R.; McKinney, J.C.; Johnson, M.D.; Doleman, S.S. Probing the Magnetic Field Structure in Sgr A* on Black Hole Horizon Scales with Polarized Radiative Transfer Simulations. *Astrophys. J.* **2017**, *837*, 180. [[CrossRef](#)]
104. Psaltis, D.; Özel, F.; Chan, C.-K.; Marrone, D.P. A General Relativistic Null Hypothesis Test with Event Horizon Telescope Observations of the Black Hole Shadow in Sgr A*, *Astrophys. J.* **2015**, *814*, 115.
105. Keitel, D.; Forteza, X.J.; Husa, S.; London, L.; Bernuzzi, S.; Harms, E.; Nagar, A.; Hannam, M.; Khan, S.; Pürrer, M.; et al. The most powerful astrophysical events: Gravitational-wave peak luminosity of binary black holes as predicted by numerical relativity. *Phys. Rev. D* **2017**, *96*, 024006. [[CrossRef](#)]

106. Centrella, J.; Baker, J.G.; Kelly, B.J.; van Meter, J.R. Black-hole binaries, gravitational waves, and numerical relativity. *Rev. Mod. Phys.* **2010**, *82*, 3069. [[CrossRef](#)]
107. Sperhake, U. The numerical relativity breakthrough for binary black holes. *Class. Quantum Gravity* **2015**, *32*, 124011. [[CrossRef](#)]
108. Baker, J.G.; Centrella, J.; Choi, D.-I.; Koppitz, M.; van Meter, J. Gravitational-Wave Extraction from an Inspiral Configuration of Merging Black Holes. *Phys. Rev. Lett.* **2006**, *96*, 111102. [[CrossRef](#)]
109. Brüggmann, B.; Tichy, W.; Jansen, N. Numerical Simulation of Orbiting Black Holes. *Phys. Rev. Lett.* **2004**, *92*, 211101. [[CrossRef](#)]
110. Campanelli, M.; Lousto, C.O.; Marronetti, P.; Zlochower, Y. Accurate Evolutions of Orbiting Black-Hole Binaries without Excision. *Phys. Rev. Lett.* **2006**, *96*, 111101. [[CrossRef](#)]
111. Pretorius, F. Evolution of Binary Black-Hole Spacetimes. *Phys. Rev. Lett.* **2005**, *95*, 121101. [[CrossRef](#)]
112. Alcubierre, M.; Bengert, W.; Brüggmann, B.; Lanfermann, G.; Nergler, L.; Seidel, E.; Takahashi, R. 3D Grazing Collision of Two Black Holes. *Phys. Rev. Lett.* **2001**, *87*, 271103. [[CrossRef](#)]
113. Diener, P.; Herrmann, F.; Pollney, D.; Schnetter, E.; Seidel, E.; Takahashi, R.; Thornburg, J.; Ventrella, J. Accurate Evolution of Orbiting Binary Black Holes. *Phys. Rev. Lett.* **2006**, *96*, 121101. [[CrossRef](#)]
114. Bishop, N.T.; Rezzolla, L. Extraction of gravitational waves in numerical relativity. *Living Rev. Relat.* **2016**, *19*, 2. [[CrossRef](#)]
115. Löffler, F.; Faber, J.; Bentivegna, E.; Bode, T.; Diener, P.; Haas, R.; Hinder, I.; Mundim, B.C.; Ott, C.D.; Schnetter, E.; et al. The Einstein Toolkit: A community computational infrastructure for relativistic astrophysics. *Class. Quantum Gravity* **2012**, *29*, 115001. [[CrossRef](#)]
116. Mösta, P.; Mundim, B.C.; Faber, J.A.; Haas, R.; Noble, S.C.; Bode, T.; Löffler, F.; Ott, C.D.; Reisswig, C.; Schnetter, E. GRHydro: A new open-source general-relativistic magnetohydrodynamics code for the Einstein toolkit. *Class. Quantum Gravity* **2014**, *31*, 015005. [[CrossRef](#)]
117. Jani, K.; Healy, J.; Clark, J.A.; London, L.; Laguna, P.; Shoemaker, D. Georgia tech catalog of gravitational waveforms. *Class. Quantum Gravity*, **2016**, *33*, 204001. [[CrossRef](#)]
118. Healy, J.; Lousto, C.O.; Zlochower, Y.; Campanelli, M. The RIT binary black hole simulations catalog. *Class. Quantum Gravity* **2017**, *34*, 224001. [[CrossRef](#)]
119. Abbott, B.P.; Abbott, R.; Abbott, T.D.; Abernathy, M.R.; Acernese, F.; Ackley, K.; Adams, C.; Adams, T.; Addesso, P.; Adhikari, R.X.; et al. Observation of Gravitational Waves from a Binary Black Hole Merger. *Phys. Rev. Lett.* **2016**, *116*, 061102. [[CrossRef](#)]
120. Abbott, B.P.; Abbott, R.; Abbott, T.D.; Abernathy, M.R.; Acernese, F.; Ackley, K.; Adams, C.; Adams, T.; Addesso, P.; Adhikari, R.X.; et al. Properties of the Binary Black Hole Merger GW150914. *Phys. Rev. Lett.* **2016**, *116*, 241102. [[CrossRef](#)]
121. Hannam, M.; Schmidt, P.; Bohé, A.; Haegel, L.; Husa, S.; Ohme, F.; Pratten, G.; Pürrer, M. Simple Model of Complete Precessing Black-Hole-Binary Gravitational Waveforms. *Phys. Rev. Lett.* **2014**, *113*, 151101. [[CrossRef](#)]
122. Taracchini, A.; Buonanno, A.; Pan, Y.; Hinderer, T.; Boyle, M.; Hemberger, D.A.; Kidder, L.E.; Lovelace, G.; Mroué, A.H.; Pfeiffer, H.P.; et al. Effective-one-body model for black-hole binaries with generic mass ratios and spins. *Phys. Rev. D* **2014**, *89*, 061502. [[CrossRef](#)]
123. Shibata, M.; Uryu, K. Simulation of merging binary neutron stars in full general relativity: $\Gamma=2$ case. *Phys. Rev. D* **2000**, *61*, 064001. [[CrossRef](#)]
124. Shibata, M.; Taniguchi, K.; Uryu, K. Merger of binary neutron stars of unequal mass in full general relativity. *Phys. Rev. D* **2003**, *68*, 084020. [[CrossRef](#)]
125. Shibata, M.; Taniguchi, K.; Uryu, K. Merger of binary neutron stars with realistic equations of state in full general relativity. *Phys. Rev. D* **2005**, *71*, 084021. [[CrossRef](#)]
126. Özel, F.; Freire, P. Masses, Radii, and the Equation of State of Neutron Stars. *Ann. Rev. Astron. Astrophys.* **2016**, *54*, 401. [[CrossRef](#)]
127. Steiner, A.W.; Lattimer, J.M.; Brown, E.F. The Neutron Star Mass-Radius Relation and the Equation of State of Dense Matter. *Astrophys. J. Lett.* **2013**, *765*, L5. [[CrossRef](#)]
128. Hotokezaka, K.; Kyutoku, K.; Okawa, H.; Shibata, M.; Kiuchi, K. Binary neutron star mergers: Dependence on the nuclear equation of state. *Phys. Rev. D* **2011**, *83*, 124008. [[CrossRef](#)]

129. Radice, D.; Bernuzzi, S.; Del Pozzo, W.; Roberts, L.F.; Ott, C.D. Probing Extreme-density Matter with Gravitational-wave Observations of Binary Neutron Star Merger Remnants. *Astrophys. J. Lett.* **2017**, *842*, L10. [[CrossRef](#)]
130. Bernuzzi, S.; Dietrich, T.; Nagar, A. Modeling the Complete Gravitational Wave Spectrum of Neutron Star Mergers. *Phys. Rev. Lett.* **2015**, *115*, 091101. [[CrossRef](#)]
131. Sekiguchi, Y.; Kiuchi, K.; Kyutoku, K.; Shibata, M.; Taniguchi, K.; Dynamical mass ejection from the merger of asymmetric binary neutron stars: Radiation-hydrodynamics study in general relativity. *Phys. Rev. D* **2016**, *93*, 124046. [[CrossRef](#)]
132. Bauswein, A.; Stergioulas, N. Unified picture of the post-merger dynamics and gravitational wave emission in neutron star mergers. *Phys. Rev. D* **2015**, *91*, 124056. [[CrossRef](#)]
133. Paschalidis, V. General relativistic simulations of compact binary mergers as engines for short gamma-ray bursts. *Class. Quantum Gravity* **2017**, *34*, 084002. [[CrossRef](#)]
134. Shibata, M.; Fujibayashi, S.; Hotokezaka, K.; Kiuchi, K.; Kyutoku, K.; Sekiguchi, Y.; Tanaka, M. Modeling GW170817 based on numerical relativity and its implications. *Phys. Rev. D* **2017**, *96*, 123012. [[CrossRef](#)]
135. Abbott, B.P.; Abbott, R.; Abbott, T.D.; Acernese, F.; Ackley, K.; Adams, C.; Adams, T.; Addesso, P.; Adhikari, R.X.; Adya, V.B.; et al. GW170817: Observation of Gravitational Waves from a Binary Neutron Star Inspiral. *Phys. Rev. Lett.* **2017**, *119*, 161101. [[CrossRef](#)]
136. Farris, B.D.; Gold, R.; Paschalidis, V.; Etienne, Z.B.; Shapiro, S.L. Binary Black-Hole Mergers in Magnetized Disks: Simulations in Full General Relativity. *Phys. Rev. Lett.* **2012**, *109*, 221102 [[CrossRef](#)]
137. Gold, R.; Paschalidis, V.; Etienne, Z.B.; Shapiro, S.L.; Pfeiffer, H.P. Accretion disks around binary black holes of unequal mass: General relativistic magnetohydrodynamic simulations near decoupling. *Phys. Rev. D* **2014**, *89*, 064060. [[CrossRef](#)]
138. Brüggmann, B. Available online: <http://www.sfb.tpi.uni-jena.de/Projects/B7.shtml> (accessed on 29 April 2019).
139. Porth, O.; Chatterjee, K.; Narayan, R.; Gammie, C.F.; Mizuno, Y.; Anninos, P.; Baker, J.G.; Bugli, M.; Chan, C.K.; Davelaar, J.; et al. The Event Horizon General Relativistic Magnetohydrodynamic Code Comparison Project. *arXiv* **2019**, arXiv:1904.04923.
140. Akiyama, K.; Alberdi, A.; Alef, W.; Asada, K.; Azulay, R.; Baczko, A.K.; Ball, D.; Baloković, M.; Barrett, J.; Bintley, D.; et al. First M87 Event Horizon Telescope Results. I. The Shadow of the Supermassive Black Hole. *Astrophys. J.* **2019**, *875*, 1.
141. Akiyama, K.; Alberdi, A.; Alef, W.; Asada, K.; Azulay, R.; Baczko, A.K.; Ball, D.; Baloković, M.; Barrett, J.; Bintley, D.; et al. First M87 Event Horizon Telescope Results. IV. Imaging the Central Supermassive Black Hole. *Astrophys. J.* **2019**, *875*, 4.



© 2019 by the author. Licensee MDPI, Basel, Switzerland. This article is an open access article distributed under the terms and conditions of the Creative Commons Attribution (CC BY) license (<http://creativecommons.org/licenses/by/4.0/>).